

System identification of ankle joint dynamics based on plane-wave ultrasound muscle imaging

Ossenkoppele, Boudewine; Daeichin, Verya; Rodriguez Hernandez, Karen; de Jong, Nico; Verweij, Martin; Schouten, Alfred; Mugge, Winfred

DOI

[10.1109/EMBC.2019.8856501](https://doi.org/10.1109/EMBC.2019.8856501)

Publication date

2019

Document Version

Final published version

Published in

2019 41st Annual International Conference of the IEEE Engineering in Medicine and Biology Society, EMBC 2019

Citation (APA)

Ossenkoppele, B., Daeichin, V., Rodriguez Hernandez, K., de Jong, N., Verweij, M., Schouten, A., & Mugge, W. (2019). System identification of ankle joint dynamics based on plane-wave ultrasound muscle imaging. In T. Penzel (Ed.), *2019 41st Annual International Conference of the IEEE Engineering in Medicine and Biology Society, EMBC 2019* (pp. 2111-2114). Article 8856501 (Proceedings of the Annual International Conference of the IEEE Engineering in Medicine and Biology Society, EMBS). IEEE.
<https://doi.org/10.1109/EMBC.2019.8856501>

Important note

To cite this publication, please use the final published version (if applicable).
Please check the document version above.

Copyright

Other than for strictly personal use, it is not permitted to download, forward or distribute the text or part of it, without the consent of the author(s) and/or copyright holder(s), unless the work is under an open content license such as Creative Commons.

Takedown policy

Please contact us and provide details if you believe this document breaches copyrights.
We will remove access to the work immediately and investigate your claim.

Green Open Access added to TU Delft Institutional Repository

'You share, we take care!' - Taverne project

<https://www.openaccess.nl/en/you-share-we-take-care>

Otherwise as indicated in the copyright section: the publisher is the copyright holder of this work and the author uses the Dutch legislation to make this work public.

System identification of ankle joint dynamics based on plane-wave ultrasound muscle imaging

Boudewine W. Ossenkopppe¹, Varya Daeichin^{1,3}, Karen E. Rodriguez Hernandez², Nicolaas de Jong^{1,3}, Martin D. Verweij^{1,3}, Alfred C. Schouten², Winfred Mugge²

Abstract—Effective treatment of movement disorders requires thorough understanding of human limb control. Joint dynamics can be assessed using robotic manipulators and system identification. Due to tendon compliance, joint angle and muscle length are not proportional. This study uses plane-wave ultrasound imaging to investigate the dynamic relation between ankle joint angle and muscle fiber stretch. The first goal is to determine the feasibility of using ultrasound imaging with system identification; the second goal is to assess the relation between ankle angle, muscle stretch, and reflex size. Soleus and gastrocnemius muscle stretches were assessed with ultrasound imaging and image tracking. For small (1° SD) continuous motions, muscle stretch was proportional to ankle angle during a relax task, but images were too noisy to make that assessment during an active position task. For transient perturbations with high velocity ($> 90^\circ/\text{s}$) the muscle length showed oscillations that were not present in the ankle angle, demonstrating a non-proportional relationship and muscle-tendon interaction. The gastrocnemius velocity predicted the size of the short-latency reflex better than the ankle angle velocity. Concluding, plane-wave ultrasound muscle imaging is feasible for system identification experiments and shows that muscle length and ankle angle are proportional during a relax task with small continuous perturbations.

I. INTRODUCTION

Many daily activities, such as standing or driving on a bumpy road, require posture maintenance. Mechanisms to resist perturbations are co-activation of antagonistic muscles and proprioceptive reflexes, originating from muscle spindles and Golgi tendon organs. Posture control experiments use both transient [1] and continuous perturbations [2]. Transients offer a straightforward assessment by isolating the instantaneous (mechanics) from the delayed (reflex) response. Continuous perturbations allow to study adaptation of reflexive and visco-elastic properties to different circumstances.

With system identification the joint dynamics can be expressed in a Frequency Response Function (FRF) from the applied torque to the measured joint angle, i.e. admittance. Motor control experiments, system identification and modelling are used to improve the understanding of the relevant structures and their interaction in posture maintenance.

The first goal of this study is to determine the feasibility of measuring muscle length changes using plane-wave ultrasound imaging during continuous and transient perturbations. The second goal is to assess the relation between ankle

rotation and muscle stretch, and their relation with the reflex response.

1) *Joint angle and muscle stretch*: Some models represent muscle length as ankle angle filtered by an elastic tendon, others assume an infinite tendon stiffness. Muscle spindles are sensitive to muscle stretch and stretch velocity. As muscle spindle stretch is derived from the joint angle, modelling muscle-tendon interaction affects the estimated muscle spindle contribution. Therefore, this study aims to verify if muscle stretch can be assumed to be proportional to ankle angle during system identification experiments.

Following transient perturbations, EMG signals show a short latency stretch reflex response (M1) and a long latency response (M2). With transient perturbations, joint velocity correlates with M1 amplitude [3]. Since muscle stretch is a more direct measure of muscle spindle input, it is hypothesized that muscle stretch velocity correlates stronger with M1 magnitude than ankle joint velocity.

II. METHOD

Eight healthy participants (5 women) aged 24-27 volunteered: four received small amplitude continuous perturbations (Experiment 1) and four received transient perturbations (Experiment 2). All participants gave informed consent and the study was approved by the human research ethics committee of the Delft University of Technology.

1) *Achilles*: A single-axis ankle manipulator (Moog, Nieuw-Vennep, The Netherlands) applied the perturbations and recorded torque and angle at 1024Hz. Participants were seated with their left foot straight (0°) and 45° knee flexion.

2) *Electromyography*: A TMSi amplifier (Porti-7) recorded EMG signals at 1024Hz. Surface electrodes were positioned according to the SENIAM guidelines on the tibialis anterior (TA), gastrocnemius medialis (GM), gastrocnemius lateralis (GL) and soleus (SOL) muscles.

3) *Ultrasound*: Images were recorded with a Verasonics Vantage 256 ultrasound system and a Philips L12-5 50mm probe operating at a centre frequency of 7.8MHz and an imaging depth of 50mm. Ultrafast ultrasound imaging uses unfocused plane-waves instead of conventional line-by-line acquisition, enabling a high temporal resolution ($> \text{kHz}$) [4]. In Experiment 1, ultrasound images were recorded at 130Hz for 23s and in Experiment 2 at 100Hz for 30s. The probe was fastened to the leg with an encasing of clay, Velcro straps and a self-adhesive bandage (Fig. 1c).

¹ Lab. of Acoustical Wavefield Imaging, TU Delft, The Netherlands.

² Dept. of Biomech. Eng., TU Delft, The Netherlands

³ Dept. of Biomed. Eng., Erasmus MC, Rotterdam, The Netherlands.
Corresponding email: B.W.Ossenkopppele@tudelft.nl

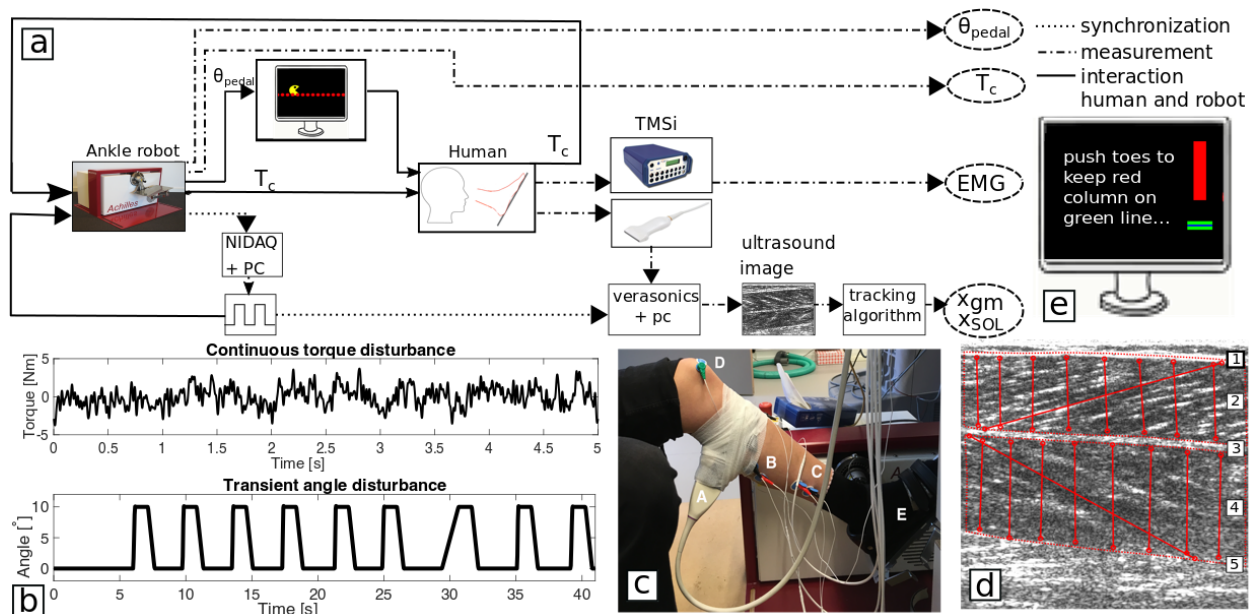


Fig. 1. *a)* Experimental setup. Human and manipulator interact through contact torque T_c . Onscreen feedback for Experiment 1: 'Pacman' shows the low-pass filtered joint angle and red dots the required angle. *b)* Top: 5s segment of the 30s continuous torque disturbance of Experiment 1. Bottom: Example of a transient position disturbance applied in Experiment 2. *c)* Attachment of ultrasound probe (A), EMG electrodes on GM (B), SOL (C) and ground electrode on knee cap (D). The foot is strapped on the pedal (E). *d)* ROIs and tracking lines in an ultrasound image. Proximal aponeurosis GM (1), ROI GM (2), distal aponeurosis GM and distal aponeurosis SOL(3), ROI SOL (4), proximal aponeurosis SOL(5). *e)* Onscreen feedback of Experiment 2. A blue bar indicates the required torque, with $\pm 5\%$ margin in green. The red column indicates the low-pass filtered torque.

4) *Data recording:* The manipulator sent a TTL signal to the TMSi and NIDAQ 6211 USB device, which sent a square wave with a pulse frequency equal to the desired ultrasound frame rate to trigger the ultrasound, see Fig. 1a.

A. Experiment 1: Continuous

1) *Signal:* The signal had equal power at 40 logarithmically spaced frequencies between 0.2Hz and 40Hz and a random phase. From 10,000 realizations, one 5s segment was chosen that had no outliers while having a distribution closest to a normal distribution, see Fig. 1b. Six repetitions formed a 30s disturbance signal.

2) *Procedure:* To ensure approximately linear dynamics during the position task, the disturbance amplitude was scaled for every participant to achieve small ankle movements (1° SD). To attain similar movements during the relax task, the virtual stiffness of the manipulator was increased. Participants performed 4 repetitions of the position task followed by 4 repetitions of the relax task, with 10-minute breaks between repetitions. During position tasks a 3Nm bias torque was applied to ensure constant contraction of the plantarflexor muscles. To allow sufficient time to achieve the initial position, disturbances started after 13s.

3) *Task:* Participants were instructed not to intervene with disturbances during the relax task. For the position task, they were instructed to keep their foot in a constant angle, while performance feedback was given onscreen (Fig. 1a).

B. Experiment 2: Transient

1) *Signal:* The transient disturbance consisted of nine Ramp-and-Hold (RaH) signals, see Fig. 1b. The first two RaHs were used to familiarize the participant with the task. Of the subsequent seven ramps, one had a velocity of $8^\circ/s$

and two ramps each had velocities of 90, 150 and $200^\circ/s$. The order was randomized and the time interval between RaHs varied ($2.5 \pm 0.29s$). The return velocity was $20^\circ/s$.

2) *Procedure:* Participants first performed 4 repetitions of the relax task with no torque requirement, then practiced the active task until they consistently maintained the required torque level of 4Nm, and finally, performed 4 repetitions of the active task. Breaks between repetitions were 10 minutes.

3) *Task:* Participants were instructed not to intervene with the disturbances during the relax task. For the active task they were instructed to contract their muscles such that the onscreen torque level was reached (Fig. 1e), but not to intervene with the disturbance.

C. Data processing

1) *Image processing:* Images were processed with the automatic tracking algorithm *Ultratrack* [5]. The algorithm is based on a Lucas-Kanade optical flow algorithm with affine optic flow extension. It tracks the complete muscle region, making it suitable for tracking larger and faster movements in which complex muscle deformations occur that can cause small regions to move out of the imaging plane. Regions of interest (ROI) for the GM and SOL were marked on the first frame, see Fig. 1d. In each ROI, a muscle fascicle was marked as well as eight points on each aponeurosis, which form vertical lines in the image. The relative movement between the eight markers on the upper and lower aponeuroses were averaged and used to determine the relative muscle stretch along the aponeurosis.

2) *Experiment 1: Continuous:* The first and last 5s segments were eliminated to remove onset and termination effects, leaving 16 segments per participant. Recordings were

transformed to the frequency domain after which the cross-spectral densities $\hat{S}_{\theta D}(f)$, $\hat{S}_{TD}(f)$, $\hat{S}_{x_{GM}D}(f)$ and $\hat{S}_{x_{SOL}D}(f)$ were determined. Here $D(f)$ is the applied torque disturbance, $T_c(f)$ the torque on the pedal and $x_{GM}(f)$ and $x_{SOL}(f)$ are the contractile element lengths of the GM and SOL muscles. Spectral densities were averaged per participant over the different trials. A closed-loop identification method was used to estimate the admittances $\hat{H}_{\theta T}(f)$, $\hat{H}_{x_{GM}T}(f)$, $\hat{H}_{x_{SOL}T}(f)$, $\hat{H}_{x_{GM}\theta}(f)$ and $\hat{H}_{x_{SOL}\theta}(f)$ by division of the spectral densities [2]. The coherence $\hat{\gamma}_{\theta D}^2(f)$ between D and θ , $\hat{\gamma}_{x_{GM}D}^2(f)$ between D and x_{GM} and $\hat{\gamma}_{x_{SOL}D}^2(f)$ between D and x_{SOL} were determined to check linearity. A coherence value of 1 indicates a linear noise-free relation. FRFs and coherences were only evaluated at the frequencies where the torque disturbance had power.

3) *Experiment 2: Transient*: Ultrasound images were analyzed with the tracking algorithm per individual ramp. For the EMG recordings 50Hz power line interference was removed, the signal was high-pass filtered (1Hz cut-off, third-order Butterworth), rectified and smoothed with a low-pass filter (80Hz cut-off, third-order Butterworth [1]). RaH segments were removed from the analysis if the torque was not within 10% of the required torque in the 100ms before ramp onset. Trials were also excluded if the EMG peak after the ramp was not larger than the mean plus 3 times the standard deviation of the baseline EMG which was determined -500 to -100ms before the ramp onset or if a large EMG peak (within 2 standard deviations of the reflex peak) was present in the 100ms before the ramp onset. The M1 and M2 response were then quantified by the area under the EMG signal at a window of 40-65ms and 70-110ms respectively and normalized with respect to the baseline EMG.

4) *Statistics*: The Pearson correlation coefficient was used to examine relationships between muscle velocity, disturbance velocity and reflex size. Significance level: $p < 0.05$.

III. RESULTS

A. Experiment 1: Continuous

1) *Feasibility*: Fig. 2 shows the ankle angle and contractile length of the GM averaged over all 16 data segments for a typical subject. During the relax task the contractile length of the GM oscillates in a similar pattern as the ankle angle and the trajectory is only slightly less smooth than the ankle angle. During the position task the x_{GM} has small high-frequency oscillations that are not present in the ankle angle. The same was observed for the x_{SOL} recording (not shown).

2) *Proportionality*: Fig. 2 shows that ankle angle is not proportional to muscle length during the position task.

Frequency domain identification: Fig. 2 shows typical results for frequency response functions $\hat{H}_{\theta T}$, $\hat{H}_{x_{GM}T}$, $\hat{H}_{x_{SOL}T}$ and coherences $\hat{\gamma}_{\theta D}^2$, $\hat{\gamma}_{x_{GM}D}^2$ and $\hat{\gamma}_{x_{SOL}D}^2$ for the position task. Before calculating the FRFs x_{SOL} and x_{GM} recordings were detrended to correct for drift and 16 out of 64 segments of the position task were removed as they showed 'jumps'.

Fig. 3 shows that overall $\hat{H}_{x_{GM}\theta}$ and $\hat{H}_{x_{SOL}\theta}$ are not constant across all frequencies, indicating that muscle length is not proportional to ankle angle. Yet, at frequencies where

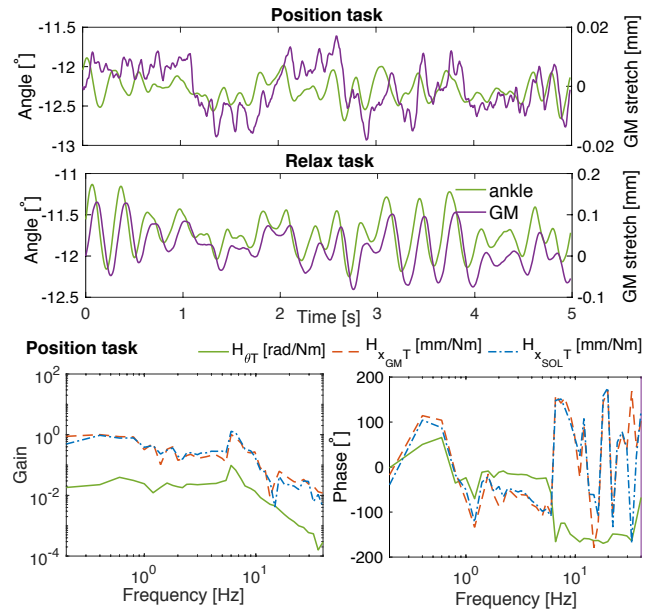


Fig. 2. Experiment 1: *Top*) Typical average ankle angle and GM contractile length during a position and relax task. *Bottom*) Typical results for frequency response functions during the position task showing similar shapes.

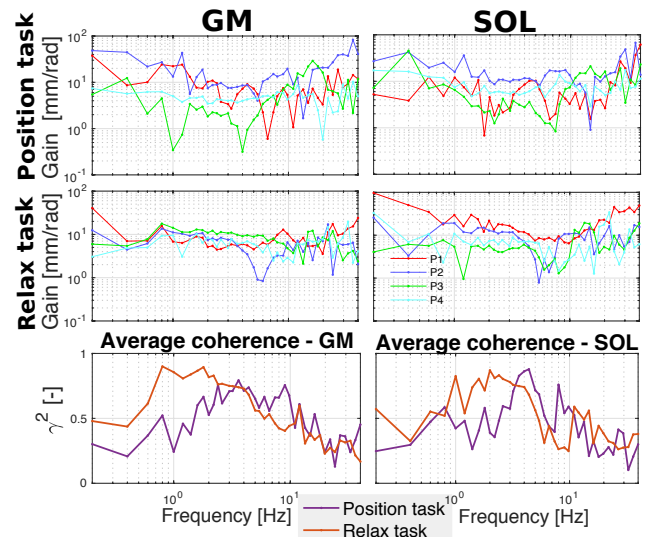


Fig. 3. Experiment 1: *Top and Middle*) If θ_{pedal} is proportional to x_{SOL} and x_{GM} then $\hat{H}_{x_{GM}\theta}$ and $\hat{H}_{x_{SOL}\theta}$ would be constant across all frequencies (colours represent subjects). *Bottom*) Average coherence for each muscle.

$\hat{\gamma}_{x_{GM}D}^2$ and $\hat{\gamma}_{x_{SOL}D}^2$ are relatively high, $\hat{H}_{x_{GM}\theta}$ and $\hat{H}_{x_{SOL}\theta}$ are relatively straight especially for the relax task. The coherence of the muscle length is much lower than that of the ankle angle, which, averaged over all frequencies and participants, is 0.98 during the relax task and 0.89 during the position task. $\hat{\gamma}_{x_{GM}D}^2$ and $\hat{\gamma}_{x_{SOL}D}^2$ are higher during the relax task than the position task especially from 1-4Hz.

B. Experiment 2: Transient

1) *Feasibility*: Fig. 4 shows a large dissimilarity between ankle angle and contractile element trajectories.

2) *Proportionality*: Fig. 4 shows that muscle length is not proportional to ankle angle during an active task, as oscillations in the GM length are missing in the ankle angle.

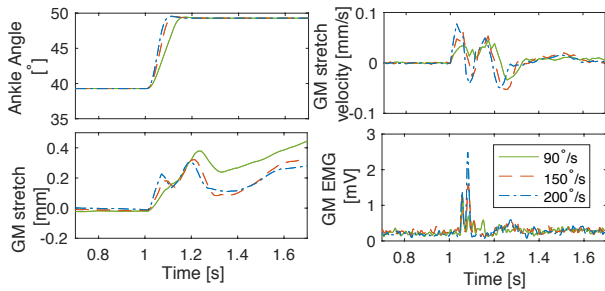


Fig. 4. Experiment 2: Response of a typical subject to RaH perturbations of different velocities during an active task, averaged over the included trials. GM contractile length shows oscillations not present in the ankle angle recording. Larger perturbation velocity corresponds with a larger GM stretch velocity and with higher peaks in the EMG trajectories.

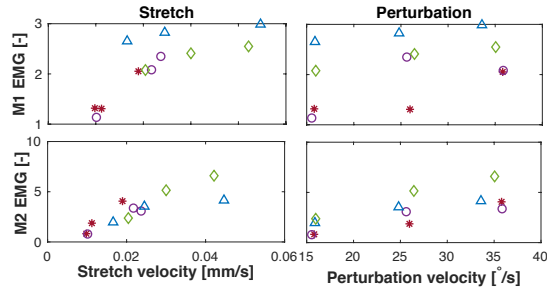


Fig. 5. Experiment 2: Average GM stretch velocity and perturbation velocity at 0.014s after perturbation onset plotted against the average M1 and M2 responses during the active task. Every symbol represents a participant. For a perfect correlation the symbols would lie on a straight line.

The same was observed for the relax task and the soleus muscle (not shown).

3) *Reflexes*: Fig. 4 shows the averaged ramp responses for a typical subject. Higher ramp velocity corresponds with a larger muscle velocity directly after ramp onset (0.014s after the disturbance) and a larger EMG peak. Fig. 5 shows the relationship of M1 and M2 with muscle stretch and perturbation velocity for all participants during the active task. M1 has a strong and significant correlation with GM muscle stretch velocity whereas no significant correlation is found with perturbation velocity (Table I). For the active condition, M2 has a strong and significant correlation with stretch and perturbation velocity. For the soleus only a strong correlation is found between perturbation velocity and M2. For the relax task, a weak correlation is found between perturbation velocity and the M1 response of the soleus. Stronger correlations are found between perturbation velocity and M2 of the GM and between GM stretch velocity and M2.

IV. DISCUSSION

1) *Feasibility*: Plane-wave ultrasound has been used before to image skeletal muscle [4]. In contrast to this study, local instead of global muscle displacement was recorded and electrical stimulation was used instead of mechanical perturbations. The high coherence between disturbance torque

and pedal angle indicates that these measurements have a low noise level. The lower coherence of muscle length, especially during the position task, may be caused by non-linear behaviour or noise in the muscle imaging. Drift was observed in some muscle length recordings. This can be due to error accumulation of the tracking algorithm, or be the behaviour of the muscle. If a subject slowly increases the level of co-activation, this will reduce muscle length.

2) *Reflex prediction*: The M1 response originates from the monosynaptic Ia afferent reflex pathway, where the Ia afferent provides feedback on muscle stretch velocity. This study found a strong correlation between muscle stretch velocity of the GM and the size of M1. However, Cronin et al. [6] previously found a weak correlation between muscle stretch velocity and the size of M1. Reasons that could explain this discrepancy are differences in measurement intervals after perturbation onset, disturbance parameters and use of change along the aponeurosis instead of fascicle velocity. The origin of the M2 response is still unclear. Nevertheless, the findings of this study align with Thilmann et al. [3] who found an increase in the size of the M2 response of the triceps surae with increased disturbance velocity.

3) *Experimental considerations*: A 0.14s lag of the data in Experiment 2, was corrected by realignment. The use of ultrafast ultrasound imaging with frame rates in the order of kHz was not explored, since RAM storage enabled recording <3000 frames consecutively. However, plane-wave ultrasound imaging allows imaging at >kHz without affecting image quality. Thus, it is possible to investigate the muscle response even shorter after the disturbance onset.

In conclusion, plane-wave ultrasound muscle length measurements in motor control experiments are feasible. With continuous perturbations, system identification on muscle length showed that muscle length and ankle angle are proportional during a relax task. For transient perturbations muscle length and ankle angle were not proportional; a stronger correlation was found between reflex response and gastrocnemius muscle stretch velocity than with ramp velocity.

REFERENCES

- [1] J. Schuurmans, E. De Vlugt, A. C. Schouten, C. G. M. Meskers, J. H. De Groot, and F. C. T. Van Der Helm, "The monosynaptic Ia afferent pathway can largely explain the stretch duration effect of the long latency M2 response," *Exp. Brain Res.*, vol. 193, no. 4, pp. 491–500, 2009.
- [2] F. C. T. Van Der Helm, A. C. Schouten, E. De Vlugt, and G. G. Brouwn, "Identification of intrinsic and reflexive components of human arm dynamics during postural control," *J. Neurosci. Methods*, vol. 119, no. 1, pp. 1–14, 2002.
- [3] A. F. Thilmann, M. Schwarz, R. Topper, S. J. Fellows, and J. Noth, "Different mechanisms underlie the long-latency stretch reflex response of active human muscle at different joints." *J. Physiol.*, vol. 444, pp. 631–643, 1991.
- [4] T. Deffieux, J. L. Gennisson, M. Tanter, M. Fink, and A. Nordez, "Ultrafast imaging of in vivo muscle contraction using ultrasound," *Appl. Phys. Lett.*, vol. 89, no. 18, 2006.
- [5] D. J. Farris and G. A. Lichtwark, "UltraTrack: Software for semi-automated tracking of muscle fascicles in sequences of B-mode ultrasound images," *Comput. Methods Programs Biomed.*, vol. 128, pp. 111–118, 2016.
- [6] N. J. Cronin, T. Rantalainen, and J. Avela, "Triceps surae fascicle stretch is poorly correlated with short latency stretch reflex size," *Muscle and Nerve*, vol. 52, no. 2, pp. 245–251, 2015.

TABLE I
CORRELATIONS AND (P - VALUE)

	GM Active	SOL Active	GM Passive	SOL Passive
Stretch Vel. - M1	0.664 (0.018)	0.441 (0.151)	0.323 (0.306)	0.492 (0.104)
Stretch Vel. - M2	0.893 (0.000)	0.540 (0.070)	0.746 (0.005)	0.444 (0.148)
Pert. Vel.- M1	0.402 (0.195)	0.430 (0.163)	0.556 (0.061)	0.585 (0.046)
Pert. Vel.- M2	0.760 (0.004)	0.903 (0.000)	0.697 (0.012)	0.277 (0.383)